İSTANBUL UNIVERSITY PRESS

European Journal of Biology

European Journal of Biology,
EJB 2025, 84 (1): 52–61

https://doi.org/10.26650/EurJBiol.2025.1560097
Submitted: 02.10.2024
Revision Requested: 19.11.2024
Last Revision Received: 15.01.2025
Accepted: 15.01.2025
Published Online 18.03.2025

Research Article

Open Access

Molecular Docking and Molecular Dynamics Analyses of Pazopanib with VEGF Receptors

Alev Er [1], Zeynep Cicek Onem [1], Sefa Celik [1], Aysen Ozel [1] & Sevim Akyuz [2]

[1] Istanbul University, Faculty of Science, Physics Department, Istanbul, Türkiye
[2] Istanbul Kultur University, Faculty of Science and Letters, Physics Department, Istanbul, Türkiye

Abstract

Objective: The antineoplastic agent Pazopanib is effective for treating renal cell cancer and soft tissue sarcoma. The aim of this study was to elucidate the anticancer mechanism of Pazopanib by exploring its molecular interactions with vascular endothelial growth factor receptors (VEGFRs). For this purpose, the most stable structure was determined, and molecular docking and molecular dynamics calculations of Pazopanib with VEGFR1 and VEGFR2 receptors were performed.

Materials and Methods: Conformational analysis of Pazopanib was performed using VegaZZ software. Pazopanib was docked to the active sites of the VEGFR1 and VEGR2 receptors (PDB IDs: 3HNG; 3VHE) using Autodock Vina software. The molecular dynamics (MD) simulations were carried out using the YASARA v22.9.24 program with the AMBER14 force field. The anticancer, antibacterial, antifungal, and antiviral activities of the compounds were predicted using PaccMann, AntiBac-Pred, AntiFun-Pred, and AntiVir-Pred.

Results: The molecular docking analysis of the Pazopanib molecule with the VEGFR1 and VEGFR2 receptors revealed a strong binding affinity of the investigated molecule towards the targets. The MD simulations, performed for Pazopanib-VEGFR1 and Pazopanib-VEGFR2 complexes showed that each docking complex and intermolecular interactions were stable throughout the simulations.

Conclusion: Molecular docking simulations revealed a strong binding affinity of Pazopanib towards VEGFR1 (-8.6 kcal/mol) and VEGFR2 (-9.9 kcal/mol), indicating its efficacy in cancer treatment. During the 40-ns MD simulation of the Pazopanib-3hng and Pazopanib-3vhe complexes, we validated the stability of Pazopanib in the active sites of the receptors. The predicted anticancer, antibacterial, antifungal, and antiviral activities of Pazopanib revealed its versatile bioactivity.

Keywords Pazopanib · VEGFR1 · VEGFR2 · Molecular docking · Molecular dynamics

Citation: Er, A., Onem, Z. C., Celik, S., Ozel, A. & Akyuz, S. Molecular Docking and Molecular Dynamics Analyses of Pazopanib with VEGF Receptors. Eur J Biol. 2025; 84(1): 52-61. DOI: 10.26650/EurJBiol.2025.1560097

Corresponding author: Sefa Celik scelik@istanbul.edu.tr

INTRODUCTION

Pazopanib, the third tyrosine kinase inhibitor approved by the Food and Drug Administration (FDA), has been authorised for the treatment of advanced or metastatic renal cell carcinoma, targeting the sixth molecular pathway. The mechanism of action involves the inhibition of intracellular tyrosine kinase activity of the vascular endothelial growth factor receptor (VEGFR), thereby exerting its therapeutic effect against renal cell carcinoma. The antiangiogenic properties of Pazopanib are responsible for its mechanism of action against advanced renal cell carcinoma. Pazopanib inhibits the intracellular tyrosine kinase portion of three VEGFR subtypes and two platelet-derived growth factor receptor (PDGFR) subtypes on endothelial cells.[1] Pazopanib has proven to be effective at slowing down tumour growth across different types of cancers. It's like a multitasking pro when it comes to targeting tumors.[2] Vascular endothelial growth factor (VEGF) positively regulates vascular endothelial cells, and the activity of VEGF is regulated by VEGFR1, VEGFR2, and VEGFR3.[3-5] VEGFR inhibitors are used for the therapy of many cancer types, especially metastatic renal cell carcinoma, and it was found in high concentrations in various cancers.[6,7] In a study conducted by Demirtas in 2013, it was observed that it showed antiproliferative and antiangiogenic effects with an increase in Pazopanib concentration in A549 and HUVEC cell lines.[8] Pazopanib is an inhibitor used in the treatment of metastatic sarcoma. It has been observed that the success rate is increased in patients with low tumour grade and especially in those with few metastatic foci. It was also found that it would be more appropriate to apply the treatment as a 2nd or 3rd line. The applicability of pazopanib should be evaluated in the patient group that has these factors.[9]

The pazopanib molecule is the first and only tyrosine kinase inhibitor currently confirmed as the second-step treatment for multiple subtypes of soft tissue sarcoma after determining the insufficiency of standard chemotherapy.[10,11] A preclinical study, originally improved as a small-molecule inhibitor of VEGFRs, demonstrated that the Pazopanib molecule has an anticancer effect.[11] Renal cell carcinoma is the most common type of kidney cancer. Africa and the Pacific islands have lower incidences of renal cell carcinoma than advanced nations, except for advanced countries in North America and Europe. Australia has a higher prevalence than other advanced countries.[12] Renal cell carcinoma cytotoxic therapy is naturally radiation-resistant or hormone therapy.[13] Pazopanib was approved by the FDA for the treatment of renal cell carcinoma and is one of the small molecules that inhibits three VEGFRs, which are named VEGFR1, VEGFR2, and VEGFR3, which are members of the receptor type tyrosine kinase.[14] VEGFR1 regulates monocyte and macrophage migration, and VEGFR2 is the based on receptor of blood vascular endothelial cells.[15,16] VEGF, a key proangiogenic molecule, plays a critical role in tumour angiogenesis and lymphangiogenesis, processes that are closely associated with tumour growth and metastasis.[17] First, the most stable conformer of the Pazopanib molecule was found, and second, in molecular docking calculations of the Pazopanib molecule, the conformer was taken as the initial geometry, and molecular docking calculations were performed with VEGFR1 and VEGFR2 receptors separately in the present study.

MATERIALS AND METHODS

Compound Selection and Preparation

The Protein Data Bank provided the 3D molecular structures of VEGFR1 (3HNG) and VEGFR2 (3VHE).

Conformational Analysis

Conformational analysis of the Pazopanib molecule (PubChem CID 10113978) was performed using VegaZZ 3.1.1 software.[18-20] This molecule's structure is optimised using AMMP with Gasteiger charges and an OPLS force field. A conjugate gradient optimiser model with 3000 steps, 0.01 Toler, and 0 steepest steps was used for the optimisation process. Then, five flexible torsion and a 1000-step Boltzmann jump conformation were selected. The parameters and their values used for conformation analysis are as follows: temperature = 298.15 K, dielectric constant = 1, long-range cutoff 15 Å, short-range cutoff 6 Å, and torsion root square difference = 60°.

Molecular Docking

The likely receptor surface binding sites were identified using CAVER software.[21] The selected active sites were subjected to molecular docking simulations using AutoDock-Vina software.[22] By removing water molecules and adding polar hydrogens, VEGFR1 and VEGFR2 were prepared for docking. The Kollman charges of the receptors were also calculated. The gas-phase optimised Pazopanib molecule was adapted for molecular docking. Furthermore, the active sites of the enzymes were determined within the 40 Å × 40 Å × 40 Å grid size, and the partial charges of the Pazopanib molecule were computed using the Geistenger technique.

Molecular Dynamics (MD)

MD simulations of the Pazopanib-3hng and Pazopanib-3vhe complexes determined by molecular docking were performed using the YASARA v22.9.24 program[23] through the AMBER14 force field[24] by docking into a water box. Periodic boundary conditions were applied, and the partial atomic charges of

the ligands were calculated using the AM1-BCC model in the YASARA program.[25] Na^+ and Cl^- ions were added to the system to neutralise the charges. The equilibrium system was created under the conditions of 0.9% NaCl, 1 bar pressure, pH 7.4, and water solvent (0.997 g/mL) at 300 K. Berendsen[26] and Particle Mesh Ewald thermostats[27] were chosen to regulate the system's pressure and temperature. Following MD simulation, the radius of gyration, root mean square deviation (RMSD), root mean square fluctuation (RMSF), and three-dimensional structural data were collected for additional analysis.

RESULTS

Conformational Analysis

After examining the conformation of Pazopanib in detail and identifying its configuration, as depicted in Figure 1; the optimised geometry parameters are presented in Table 1. The C-C bond lengths of the phenyl group of Pazopanib and the chromene derivative[28] were calculated in the range of 1.341-1.495 Å and 1.394-1.400 Å, respectively. In the crystal structures of the bisbenzylisoquinoline alkaloid methylwariftein[29] and benzene[30], the bond lengths of the phenyl groups were in the range of 1.360-1.412 Å, and 1.374-1.382 Å, respectively.

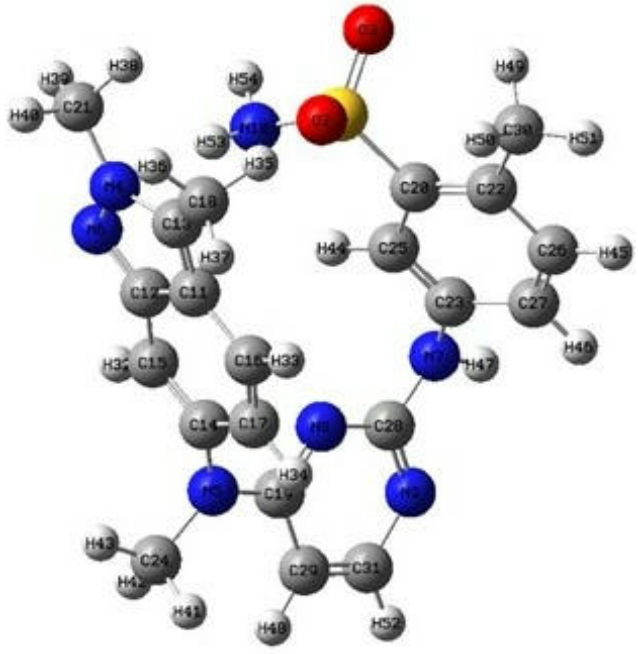

Figure 1. Conformational analysis of the Pazopanib molecule revealed the molecular structure of its most stable conformer.

Table 1. The optimised geometry parameters of Pazopanib were determined by conformational analysis (bond lengths in Å).

Atoms		Atoms		Atoms		Atoms	
S1-O2	1.501	C26-H45	1.088	C24-H41	1.114	C13-C11	1.317
S1-O3	1.502	C27-H46	1.088	C24-H42	1.115	C11-C12	1.443
S1-N10	1.593	C25-H44	1.092	C24-H43	1.115	N4-C21	1.456
N10-H53	0.993	C23-N7	1.377	N5-C14	1.386	C21-H38	1.114
N10-H54	0.99	N7-H47	0.999	C14-C15	1.354	C21-H39	1.113
S1-C20	2.8126	N7-C28	1.376	C15-H32	1.088	C21-H40	1.113
C20-C22	1.356	C28-N9	1.303	C15-C12	1.473	C13-C18	1.5
C22-C26	1.488	N9-C31	1.437	C12-C11	1.443	C18-H35	1.113
C26-C27	1.341	C31-H52	1.089	C11-C16	1.473	C18-H36	1.112
C27-C23	1.481	C31-C29	1.341	C16-C17	1.348	C18-H37	1.113
C23-C25	1.349	C29-H48	1.086	C17-C14	1.501		
C20-C25	1.495	C29-C19	1.492	C16-H33	1.088		
C22-C30	1.8629	C19-N8	1.311	C17-H34	1.089		
C30-H49	1.113	N8-C28	1.439	C12-N6	1.311		
C30-H50	1.113	N5-C19	1.399	N6-N4	1.407		
C30-H51	1.113	N5-C24	1.477	N4-C13	1.435		

Molecular Docking Calculations

Pazopanib showed strong efficacy against all human VEGFRs and exhibited anticancer activity in a range of human tumour xenografts, such as lung, breast, and renal cell carcinoma.[31–35] Using molecular docking calculations, the binding of Pazopanib to VEGFR1 and VEGFR2 was examined to elucidate the drug's mechanism of action. AutoDockVina was used to perform the molecular docking computations.[22] Docking was possible with the crystal structures of VEGFR1 and VEGFR2, which were obtained from the Protein Data Bank (PDB ID: 3HNG, 3VHE).[36,37] After removing the H_2O molecules and placing the polar hydrogens, the Kollman charges of VEGFR1 and VEGFR2 were determined. The partial charges of pazopanib were calculated using the Geistenger approach, and the active sites of VEGFR1 and VEGFR2 were derived in grid size 40 Å×40 Å×40 Å.

Because of the calculations, the binding affinity of Pazopanib docked with VEGFR1 was -8.6 kcal/mol. 3D docking representations of Pazopanib in the active site of VEGFR1 are presented in Figure 2. Interactions between VEGFR1 and Pazopanib are as follows: Pi-alkyl with a length of 4.72 Å between Pazopanib and Ile881; pi-alkyl with a length of 4.97 Å and alkyl with a length of 5.28 Å with Leu882; alkyl with a length of 5.28 Å with Ile885; alkyl with a length of 5.17 Å with Val891; alkyl with a length of 4.77 Å with Leu1013; pi-sulfur with a length of 5.38 Å with Cys1018; H bond with a length of 2.48 Å with His1020; pi-alkyl with lengths of 5.46 Å, 5.50 Å and H bond with length of 2.58 Å with Arg1021; H bond with a length of

2.55 Å and pi-anion with lengths of 4.52 Å, 4.99 Å with Asp1040; carbon hydrogen bond with a length of 3.3 Å with Pro1062 and H bond with length of 2.87 Å with Tyr1076.

Pazopanib docked with VEGFR2 has a binding affinity of −9.9 kcal/mol, as determined from the calculations. 3D docking representations of Pazopanib in the active site of VEGFR2 are presented in Figure 3. Interactions between VEGFR2 and Pazopanib are as follows: Alkyl with length of 4.88 Å and pi-alkyl with length of 5.03 Å between Pazopanib and Leu840; pi-sigma with lengths of 3.8 Å, 3.89 Å with Val848; alkyl with length of 3.36 Å and pi-alkyl with lengths of 4.6 Å, 4.7 Å with Ala866; pi-alkyl with length of 4.91 Å and pi-cation with length of 4.45 Å and H bond with length of 2.88 Å with Lys868; pi-anion with length of 3.58 Å with Glu885; alkyl with length of 5.12 Å with Ile888; pi-alkyl with length of 5.19 Å with Leu889; pi-alkyl with length of 4.25 Å with Val899; pi-alkyl with length of 5.15 Å with Val916; pi-alkyl with length of 4.92 Å with Phe918; alkyl with length of 4.67 Å with Cys919; pi-sigma with lengths of 3.86 Å, 3.93 Å with Leu1035; pi-sulfur with length of 5.62 Å with Cys1045; unfavourable acceptor-acceptor with length of 2.92 Å and pi-anion with length of 4.75 Å and carbon hydrogen bond with length of 3.46 Å with Asp1046; pi-pi t-shaped with length of 5.14 Å with Phe1047.

The free energy of binding to biological macromolecules of small ligands is estimated using the MM/GBSA and MM/PBSA methods.[38–43] Wang[38] created software that combines

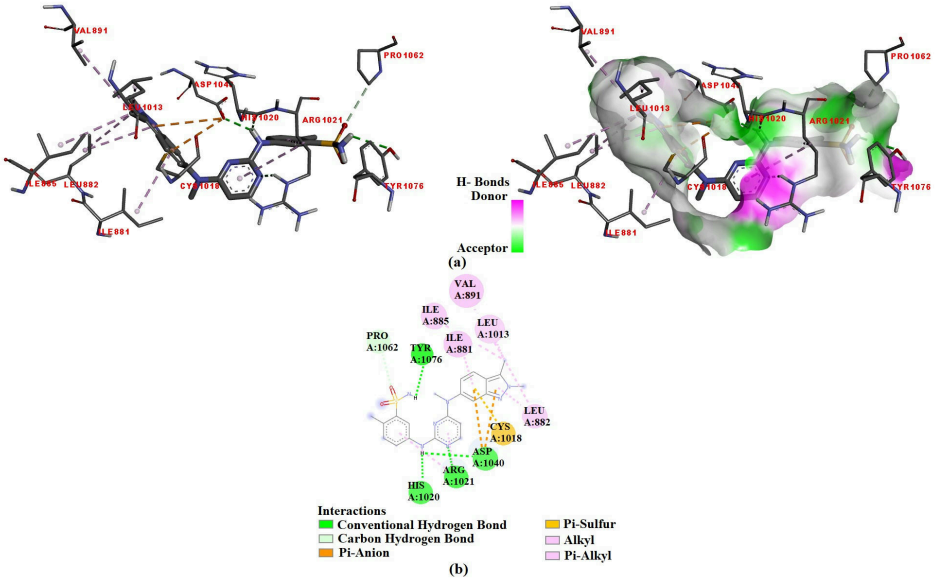

Figure 2. Pazopanib molecular docked model with VEGFR1 (a) Pazopanib and VEGFR1 interactions are indicated by coloured dashed lines (b) (ΔG = −8.6 kcal/mol).

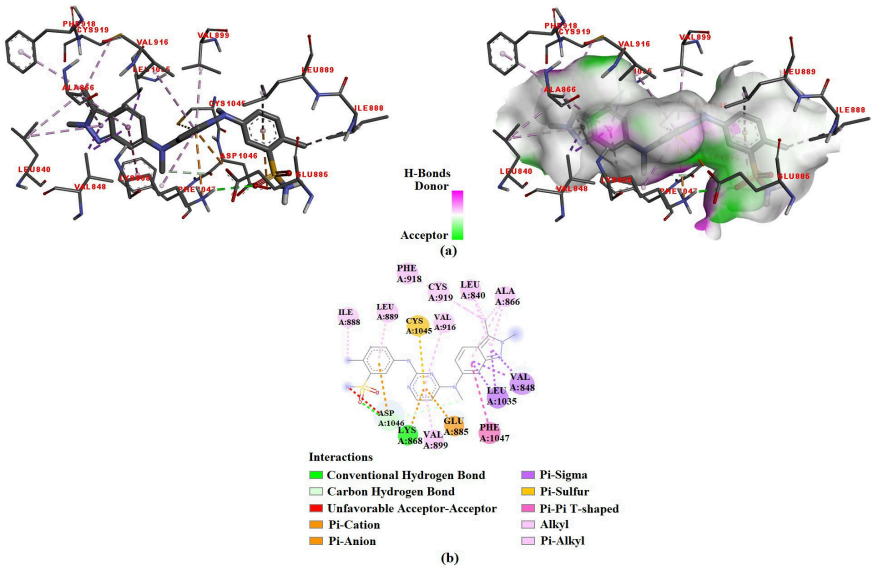

Figure 3. Pazopanib's molecular docked model with VEGFR2 (a) Pazopanib and VEGFR2 interactions are indicated by coloured dashed lines (b) (ΔG = −9.9 kcal/mol).

both methodologies, known as the MM/PB(GB)SA approach, due to the importance of these two approaches. The present study used Wang's[38] software, which is based on the MM/PB(GB)SA method, to compute the free energy of binding between Pazopanib and VEGFR1 and VEGFR2. By utilising the MM/PB(GB)SA methods with the GAFF2 and ff14SB force field combination and the GB6 process, the anticipated binding free energy of Pazopanib with VEGFR1 and with VEGFR2 were found to be 29.82 and 43.44 kcal/mol, respectively.[38]

Molecular Dynamics Calculations

RMSD graphs of the Pazopanib-3hng and Pazopanib-3vhe complexes are shown in Figure 4a and Figure 4b, respectively. These figures show the RMSD values for the α-carbon atom, the backbone, and all heavy atoms in the Pazopanib-3hng and Pazopanib-3vhe complexes, respectively, across a 40 ns MD simulation. At 1.442 Å, the average Cα RMSD ranged from 0.477 Å to 2.742 Å for Pazopanib-3hng, and at 1.438 Å, the average Cα RMSD ranged from 0.38 Å to 2.044 Å for Pazopanib-3vhe. At 1.516 Å, the average backbone RMSD ranged from 0.54 Å to 2.831 Å for Pazopanib-3hng, and at 1.485 Å, the average backbone RMSD ranged from 0.43 Å to 2.075 Å for Pazopanib-3vhe. The all-heavy atom RMSD ranged from 0.62 Å to 3.262 Å, with an average of 2.037 Å for Pazopanib-3hng, and the all-heavy atom RMSD ranged from 0.506 Å to 2.65 Å, with an average of 2.026 Å for Pazopanib-3vhe.

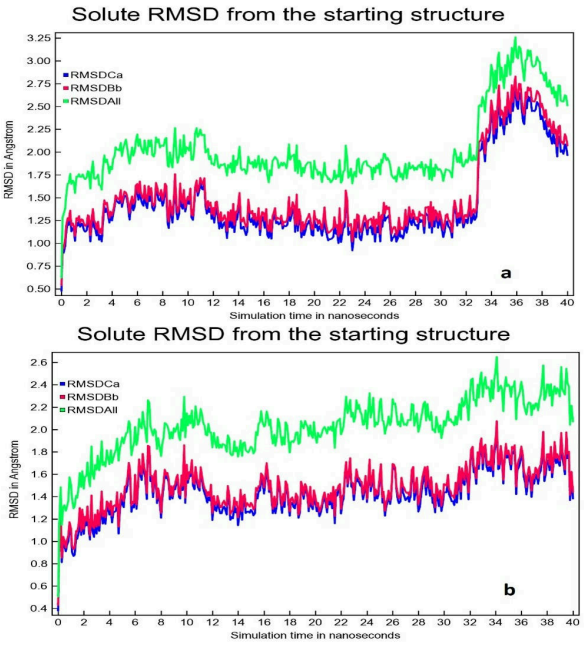

Figure 4. MD trajectory analysis of the Pazopanib-3hng (a) and Pazopanib-3vhe (b) complexes during 40 ns simulation. Protein root mean square deviation (RMSD) plot as a function of simulation time {RMSD of α-carbon atom = blue; backbone = red; and all heavy atom = green}.

The stability of the ligand-protein complex was determined by the RMSD graph deviation being less than 4 Å. RMSD graphs of the ligand in the Pazopanib-3hng and Pazopanib-3vhe complexes (Figure 5a and Figure 5b) display the degree of structural deviation of the ligand atoms during 40 ns simulations.

Figure 6a and Figure 6b display the RMSF graphs of the Pazopanib-3hng and Pazopanib-3vhe complexes. The RMSF values of the Pazopanib-3hng and Pazopanib-3vhe complexes vary in the ranges of 0.4 Å-7.36 Å and 0.39 Å-5.09 Å, respectively. For Pazopanib-3hng, Glu803 (7.36 Å), Lys991 (7.29 Å), Glu992 (5.05 Å), Val804 (4.74 Å), Pro805 (4.44 Å), Glu811 (4.18 Å), Arg812 (3.83 Å), Glu808 (3.81 Å), Pro993 (3.53 Å), Gln809 (3.04 Å), and Asp807 (3.03 Å) and for Pazopanib-3vhe, Gln1169 (5.09 Å), Leu995 (4.39 Å), Asp994 (4.18 Å), Lys997 (3.37 Å), Arg819 (3.34 Å), Tyr996 (3.17 Å), and Lys939 (3.1 Å) all showed somewhat greater fluctuations throughout the simulation. During the 40-ns MD simulation of the Pazopanib-3hng and Pazopanib-3vhe complexes, the radius of gyration (Rg) graphs is displayed in Figure 7a and Figure 7b. On average, the Rg of the Pazopanib-3hng complex is 19.571 Å and of the Pazopanib-3hng complex is 20.172 Å.

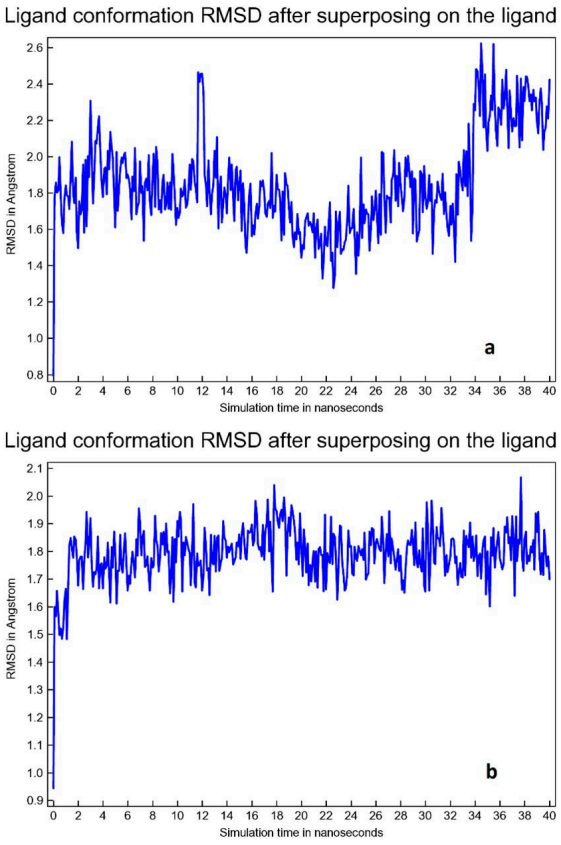

Figure 5. RMSD plots of the ligand for 3hng (a) and 3vhe (b).

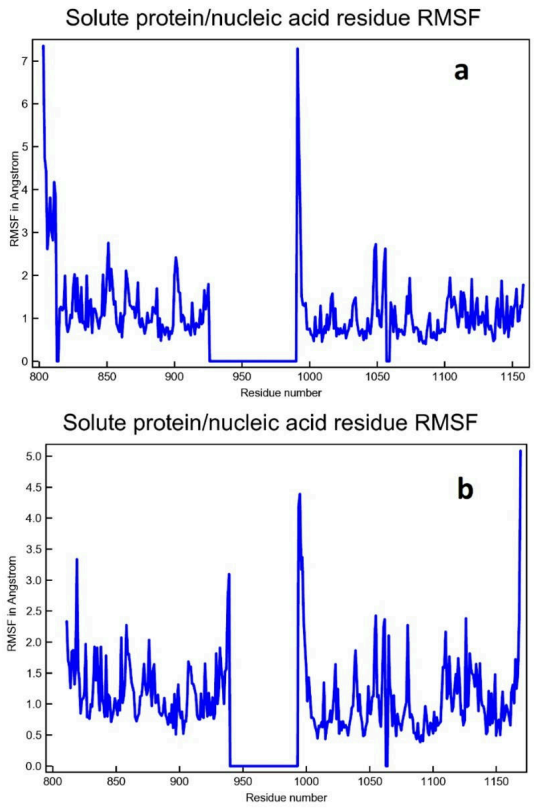

Figure 6. Mean square fluctuation (RMSF) plots of the Pazopanib-3hng (a) and Pazopanib-3vhe (b) complexes.

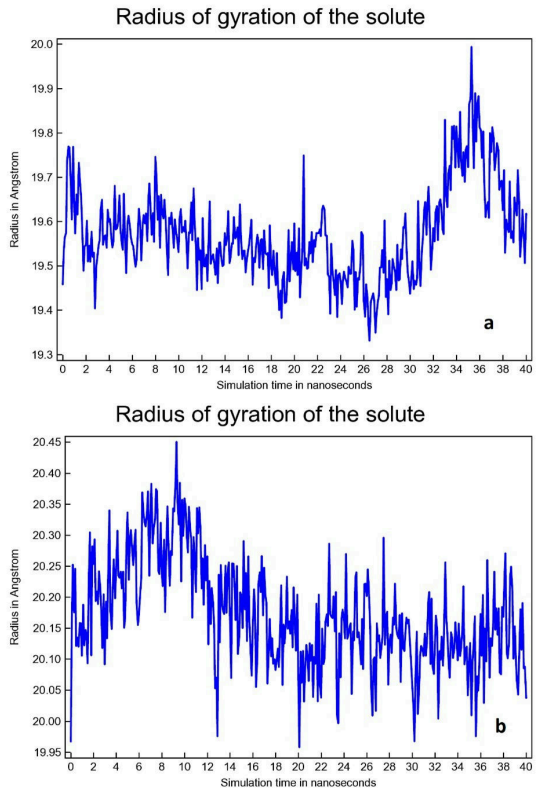

Figure 7. Radius of gyration (Rg) plots of the Pazopanib-3hng (a) and Pazopanib-3vhe (b) complexes.

Antibacterial, Antifungal, and Antiviral Activities

The antibacterial, antifungal, and antiviral activities of the compound were predicted using AntiBac-Pred, AntiFun-Pred, and AntiVir-Pred.[44-50] The probability scores of Pazopanib are presented in Table 2. According to these findings, Pazopanib may be effective against *Prevotella intermedia* (confidence: 0.1898), *Shigella flexneri* (confidence: 0.1221), *Fusobacterium nucleatum* (confidence: 0.0633), and *Staphylococcus intermedius* (confidence: 0.0320). Zaidi et al. reported the antibacterial activity of 2-(4-allylpiperazin-1-yl)-1-(1-(4-nitrophenyl)-1Htetrazol-5-yl) methanone using AntiBac-Pred.[51] For the activity against *Shigella flexneri*, the confidence value of the investigated compound was 0.0296. However, the confidence value of our molecule against *Shigella flexneri* was predicted to be 0.1221, indicating that Pazopanib should be more effective than 2-(4-allylpiperazin-1-yl)-1-(1-(4-nitrophenyl)-1Htetrazol-5-yl) ethenone.

Table 2. Probability scores of the Pazopanib.

Predicted antibacterial targets		
Name	**ChEMBL ID**	**Confidence**
RESISTANT Prevotella intermedia	CHEMBL613261	0.1898
Shigella flexneri	CHEMBL614396	0.1221
RESISTANT Fusobacterium nucleatum	CHEMBL614609	0.0633
Staphylococcus intermedius	CHEMBL614422	0.0320
Predicted antifungal activity		
Galactomyces geotrichum	CHEMBL613775	0.0780
Predicted inhibition of viral proteins		
Virus	**Protein target**	**Confidence**
Human immunodeficiency virus 1	Human immunodeficiency virus type 1 reverse transcription	0.2777
Vaccinia virus (strain Western Reserve) (VACV) (Vaccinia virus (strainWR))	DNA polymerase	0.0616

Anticancer Sensitivity Prediction

The PaccMann database was used to search for Pazopanib's anti-cancer activity against various chondrosarcoma cell lines.[52] Table 3 lists Pazopanib's anticipated anticancer properties against different cell lines. In particular, Pazopanib exhibits the highest efficacy against breast cancer (IC_{50} = 4.871).

Table 3. Anticancer activity of the compounds based on their molecular structure.

Site	Cosmic ID	Cell Line No.	Dataset	IC_{50} (log(µmol))
Breast	949093	949093	GDSC	4.871
Lung_NSCLC	908463	908463	GDSC	2.0180
Urogenital_system	930297	930297	GDSC	4.386
soft_tissue	909754	909754	GDSC	4.264
Breast	1290905	1290905	GDSC	4.241

DISCUSSION

VEGFR inhibitors are used for the therapy of many cancer types, especially metastatic renal cell carcinoma, and it was found in high concentrations in various cancers.[6,7] *In vitro*, Pazopanib showed strong efficacy against all human VEGFRs and closely related tyrosine receptor kinases. It also exhibited anticancer activity in a range of human tumour xenografts, such as lung, breast, and renal cell carcinoma.[31–35] Using molecular docking calculations, the binding of Pazopanib to VEGFR1 and VEGFR2 is examined to elucidate the drug's mechanism of action. Kuzu et al. performed molecular docking calculations using the VEGFR1 (PDB ID: 3HNG) receptor and Lenvatinib, Polydatin, Beta-Caryophyllene, and plasmotide M molecules. As a result of the calculation, Lenvatinib was assigned to ASP1040, ILE1038, LEU1013, CYS1018, HIS1020, CYS1039, LYS861, LEU882, VAL909, VAL892; Polydatin to ILE1019, VAL892, GLU878, ASP1040, CYS1018, ILE881, VAL892, ILE881, PHE1041; Beta-Caryophyllene was found to interact with LEU882, CYS1039, VAL841, LYS861, ALA861, VAL909, ALA859, VAL907; Plakortide M was obtained to interact with ARG1021, ILE1019, CYS1018, VAL909, CYS1039, VAL892, LEU882, LEU1013, ILE881, HIS1020 amino acids.[53] As a result of molecular docking calculation performed by Bharathi et al. with VEGFR1 (PDB ID: 3HNG) receptor, it was found that 5-fluorouracil interacts with VAL 892, LEU 882, GLU 878, LEU 833, TYR 914, GLY 915, LEU 1029, VAL 841, LYS 913, TYR 911, CYS 912, VAL 860, ALA 859, PHE 1041, GLY 1042, ASP 1040, CYS 1039, ILE 1038, LYS 861, VAL 907, ILE 908, VAL 909, GLU 910; Hexadecane with PHE 1041, CYS 1039, ASP 1040, ILE 1038, HIS 1020, CYS 1018, LEU 1013, ILE 885, ILE 881, LEU 882, GLU 878, ARG 1026, ARG 1045, VAL 841, VAL 891, VAL 892, LEU 833, GLY 915, ASN 916, LEU 1029, LYS 861, VAL 860, ALA 859, LYS, 913, CYS 912, TYR 911, GLU 910, VAL 909, ILE 908, VAL 907; Hexadecanoic acid, methyl ester with GLU 910, ALA 859, VAL 909, VAL 892, VAL 891, ILE 1038, TYR 911, CYS 912, ARG 835, VAL 841, LEU 833, GLY 834, ASN 919, ILE 885, LEU 1013, CYS 1018, LEU 1029, ASN 916, GLY 915, ARG 1026, GLU 811, GLU 808, ASP 807, LYS 873, ALA 874, LEU 875, THR 877, LYS 861, GLU 878, ILE 881, LEU 882, ILE 1019, ARG 1021, ASP 1046, ARG 1045, HIS 1020, CYS 1039, ASP 1040, PHE 1041, LEU1043, ALA 1044, GLY 1042; Quinoline, 1,2-dihydro-2,2,4-trimethyl- with LEU 1013, VAL 891, VAL 892, ILE 885, LEU 882, ILE 881, HIS 1020, ARG 1021, ILE 1019, CYS 1018, ASP 807, GLU 878, THR 877, LEU 875, ALA 874, LEU 1043, GLY 1042, PHE 1041, ASP 1040, CYS 1039, ILE 1038, LYS 861, VAL 841, ALA 859, SER 832, LEU 833, GLY 834, ASN 1034, TYR 1002, ASP 998, TYR 920, LYS 924, ILE 994, PRO 993, GLU 992, LYS 991, ASN 916, GLY 915, TYR 914, LYS 913, CYS 912, TYR 911, LEU 1029, LEU 1030, SER 1031 amino acids.[54] Kouassi et al. studied on the VEGFR2 (PDB ID: 3VHE) receptor found that the interacts with amino acids Glu 885, Phe 918, Cys 919, Asp 1046, Leu 840, Val 848, Ala 866, Leu 889, Val 898, Val 899, Val 916, Leu 1019, Leu 1035, Ile 1044, Cys 1045, Phe 1047 of molecule with code Z2121011596; with amino acids Glu 885, Cys 919, Asp 1046, Leu 840, Val 848, Ala 866, Ile 888, Leu 889, Val 898, Val 899, Val 916, Leu 1019, Leu 1035, Cys 1045, Phe 1047, Val 916 Phe 1047 of molecule with code PV-002089512142; and with amino acids Glu 885, Asp 1046, Leu 840, Val 848, Val 898, Val 899, Val 914, Phe 918, Cys 919, Leu 1019, Leu 1035, Ile 1044, Cys 1045, Phe 1047, Hie 1026, Asp 1046, Phe 1047 of molecule with code PV-002342843731.[55] In a study by Mendie et al. in 2022, molecular docking analysis was performed using the VEGFR2 (PDB ID: 3VHE) receptor.[56] As a result of the calculation, it was determined that H bonds with the indicated amino acids; oleanolic acid with ARG 1027 and 1LE 1044 amino acids; Panaxadiol with ARG 1027, HIS 1026, and ILE 1044 amino acids; Panaxatriol with ARG 1027, HIS 1026, and 1LE 1044 amino acids; Ursolic acid with amino acids ASP 814, ARG 1027, and ILE 1044; Hecogenin with amino acids ARG 1027, GLU 818; Dovitinib with GLU 917; Gefitinib with amino acids ASP 1046, CYS 919.[56] Based on the molecular docking data obtained in the present study and the data previously published in the literature in related studies, we concluded that the amino acids with which the Pazopanib ligand interacts with VEGFR1 (3HNG) and VEGFR2 (3VHE) are similar in our study, as can be seen in Figure 2 and Figure 3.

In 2022, a study on VEGF suggested that VEGF strengthens the endothelium's intracellular defense system by providing a strong blood vessel barrier to prevent bacterial invasion.[57] A Phase II study on Pazopanib showed anti-cancer activity in patients with previously treated metastatic breast cancer.[58] In 2015, Zhao et al. observed that Pazopanib reduced growth and survival in all NSCLC cell lines tested, including A549, YTLMC-90 and L9981 cells.[59] A study demonstrated that the combination of Sorafenib/Pazopanib with sildenafil exhibited significantly greater efficacy in preventing infection and the development of Adenovirus, Mumps, Chikungunya virus, Dengue virus, Rabies virus, West Nile virus, Yellow Fever virus, and Enterovirus 71 compared to sorafenib/pazopanib alone. Furthermore, Rafenib drugs and Pazopanib independently eradicated laboratory-cultured antibiotic-

resistant *Escherichia coli*, an effect correlated with a reduction in DNAK and RecA expression.[60] Pyrimidine-based compounds play a crucial role in drug discovery across various therapeutic areas, including anti-infective, anticancer, antiviral, antibacterial, and antifungal applications.[61-77] Given that Pazopanib is a substituted pyrimidine derivative, the findings from existing literature (as presented in Table 2 and Table 3) align with the observations reported in this study.

CONCLUSION

One antitumor drug used to treat advanced renal cell carcinoma is Pazopanib, which is an inhibitor of several receptor tyrosine kinases. The most stable conformation of Pazopanib against VEGFR1 and VEGFR2 was identified using molecular docking simulations to examine its mode of action. With binding affinities of 8.6 and 9.9 kcal/mol, respectively, Pazopanib was shown to bind to VEGFR1 and VEGFR2. Binding affinity is a critical parameter in drug design that quantifies the strength of the interaction between a ligand and its target protein. This reflects the stability and specificity of the ligand-protein complex. The effectiveness of Pazopanib in cancer treatment was demonstrated by its affinity to both VEGFR1 and VEGFR2 receptors, as predicted. Rg quantitatively describes the compactness of a protein structure. The root mean square distance of all atoms in the protein from its centre of mass. This metric provides an overall measure of the protein's spatial dimensions and structural conformation. The Rg values for the Pazopanib-3hng and Pazopanib-3vhe complexes was, on average, 19.571 Å and 20.172 Å throughout the 40-ns MD simulation. The ranges of 0.4 Å-7.36 Å and 0.39 Å-5.09 Å are the RMSF values for the Pazopanib-3hng and Pazopanib-3vhe complexes, respectively. Based on computational analyses of antibacterial and anticancer activity, Pazopanib demonstrates maximal potency against resistant *Prevotella intermedia* (confidence score: 0.1898) and breast cancer.

Ethics Committee Approval	Ethics committee approval is not required for the study.
Peer Review	Externally peer-reviewed.
Author Contributions	Conception/Design of Study- A.E., Z.C.O., S.C., A.E.O., S.A.; Data Acquisition- A.E., Z.C.O., S.C., A.E.O., S.A.; Data Analysis/Interpretation- A.E., Z.C.O., S.C., A.E.O., S.A.; Drafting Manuscript- A.E., Z.C.O., S.C., A.E.O., S.A.; Critical Revision of Manuscript- A.E., Z.C.O., S.C., A.E.O., S.A.; Final Approval and Accountability- A.E., Z.C.O., S.C., A.E.O., S.A.
Conflict of Interest	Authors declared no conflict of interest.
Financial Disclosure	Authors declared no financial support.

Author Details

Alev Er
[1] Istanbul University, Faculty of Science, Physics Department, Istanbul, Türkiye
0000-0002-3190-5342

Zeynep Cicek Onem
[1] Istanbul University, Faculty of Science, Physics Department, Istanbul, Türkiye
0000-0003-0662-0641

Sefa Celik
[1] Istanbul University, Faculty of Science, Physics Department, Istanbul, Türkiye
0000-0001-6216-1297 scelik@istanbul.edu.tr

Aysen Ozel
[1] Istanbul University, Faculty of Science, Physics Department, Istanbul, Türkiye
0000-0002-8680-8830

Sevim Akyuz
[2] Istanbul Kultur University, Faculty of Science and Letters, Physics Department, Istanbul, Türkiye
0000-0003-3313-6927

REFERENCES

1 Keisner SV, Shah SR. Pazopanib. *Drugs*. 2011;71(4):443-454.
2 Schutz FA, Choueiri TK, Sternberg CN. Pazopanib: Clinical development of a potent anti-angiogenic drug. *Crit Rev Oncol Hematol*. 2011;77(3):163-171.
3 Ferrara N. Vascular endothelial growth factor and the regulation of angiogenesis. *Recent Prog Horm Res*. 2000;55:15-35.
4 Chung AS, Ferrara N. Developmental and pathological angiogenesis. *Annu Rev Cell Dev Biol*. 2011;27:563-584.
5 Ustun E, Sahin N. Analysis of interactions of NHC type molecules and NHC-Ag complexes with VEGFR-2 and DNA: A molecular docking study. *Adiyaman Univ J Sci*. 2021;11(1):113-125.
6 Ivy SP, Wick JY, Kaufman BM. An overview of small-molecule inhibitors of VEGFR signaling. *Nat Rev Clin Oncol*. 2009;6(10):569-579.
7 Jayaraman S, Umapathy VR, Govindaraj J, Govidaraj K. Molecular docking analysis of vascular endothelial growth factor receptor with bioactive molecules from *Piper longum* as potential anti-cancer agents. *Bioinformation*. 2021;17(1):223-228.
8 Demirtas B. Küçük hücreli olmayan akciğer kanseri hücre hattında (a549) yeni bir tirozin kinaz inhibitörü olan Pazopanibin (gw786034) antianjiyojenik etkilerinin araştırılması, 2013, Yüksek Lisans Tezi, Anadolu Üniversitesi.
9 Soylemez CM. Pazopanib tedavisi alan metastatik yumuşak doku sarkomu hastalarında tedavi yanıtı ve bu durumu etkileyen faktörler, retrospektif analizi, 2021, Uzmanlık tezi, Ege Üniversitesi.
10 Van Der Graaf WT, Blay JY, Chawla SP, et al. Pazopanib for metastatic soft-tissue sarcoma (PALETTE): A randomised, double-blind, placebo-controlled phase 3 trial. *The Lancet*. 2012;379(9829):1879-1886.
11 Lee AT, Jones RL, Huang PH. Pazopanib in advanced soft tissue sarcomas. *Signal Transduct Target Ther*. 2019;4(1):1-10.
12 Ferlay J, Soerjomataram I, Dikshit R, et al. Cancer incidence and mortality worldwide: sources, methods and major patterns in GLOBOCAN 2012. *Int J Cancer*. 2015;136(5):E359-E386.
13 Sternberg CN, Davis ID, Mardiak J, et al. Pazopanib in locally advanced or metastatic renal cell carcinoma: Results of a randomized phase III trial. *J Clin Oncol*. 2010;28(6):1061-1068.
14 Li W, Feng C, Di W, et al. Clinical use of vascular endothelial growth factor receptor inhibitors for the treatment of renal cell carcinoma. *Eur J Med Chem*. 2020;200:112482. doi:10.1016/j.ejmech.2020.112482
15 Simons M, Gordon E, Claesson-Welsh L. Mechanisms and regulation of endothelial VEGF receptor signalling. *Nat Rev Mol Cell Biol*. 2016;17(10):611-625.

16 Tzima E, Irani-Tehrani M, Kiosses, et al. A mechanosensory complex that mediates the endothelial cell response to fluid shear stress. *Nature*. 2005;437(7057):426-431.

17 Hurwitz HI, Dowlati A, Saini S, et al. Phase I trial of Pazopanib in patients with advanced cancer. *Clin Cancer Res*. 2009;15(12):4220-4227.

18 Pedretti A, Villa L, Vistoli G. VEGA: A versatile program to convert, handle and visualize molecular structure on Windows-based PCs. *J Mol Graph Model*. 2002;21(1):47-49.

19 Pedretti A, Villa L, Vistoli G. Atom-type description language: A universal language to recognize atom types implemented in the VEGA program. *Theor Chem Acc*. 2003;109(4):229-232.

20 Pedretti A, Villa L, Vistoli G. VEGA–an open platform to develop chemo-bio-informatics applications, using plug-in architecture and script programming. *J Comput Aided Mol Des*. 2004;18(3):167-173.

21 Jurcik A, Bednar D, Byska J, et al. CAVER Analyst 2.0: Analysis and visualization of channels and tunnels in protein structures and molecular dynamics trajectories. *Bioinformatics*. 2018;34(20):3586-3588.

22 Trott O, Olson AJ. AutoDock Vina: Improving the speed and accuracy of docking with a new scoring function, efficient optimization, and multithreading. *J Comput Chem*. 2010;31(2):455-461.

23 Krieger E, Vriend G. YASARA View—molecular graphics for all devices—from smartphones to workstations. *Bioinformatics*. 2014;30(20):2981-2982.

24 Maier JA, Martinez C, Kasavajhala K, et al. ff14SB: Improving the accuracy of protein side chain and backbone parameters from ff99SB. *J Chem Theory Comput*. 2015;11(8):3696-3713.

25 Jakalian A, Jack DB, Bayly CI. Fast, efficient generation of high-quality atomic charges. AM1-BCC model: II. Parameterization and validation. *J Comput Chem*. 2002;23(16):1623-1641.

26 Meyer M, Pontikis V. Computer simulation in materials science: Interatomic potentials, simulation techniques and applications, Springer Science & Business Media; 2012.

27 Essmann U, Perera L, Berkowitz ML, Darden T, Lee H, Pedersen LG. A smooth particle mesh Ewald method. *J Chem Phys*. 1995;103(19):8577-8593.

28 Dlala NA, Bouazizi Y, Ghalla H, Hamdi N. DFT calculations and molecular docking studies on a chromene derivative. *J Chem*. 2021;2021(1):6674261. doi:10.1155/2021/6674261

29 Borkakoti N, Palmer RA. The structure of the bisbenzylisoquinoline alkaloid methylwarifteine. *Acta Crystallogr. B*. 1978;34(2):490-495.

30 Cox EG. Crystal structure of benzene. *Rev Mod Phys*. 1958;30(1):159. doi:10.1103/RevModPhys.30.159

31 Sloan B, Scheinfeld NS. Pazopanib, a VEGF receptor tyrosine kinase inhibitor for cancer therapy. *Curr Opin Investig Drugs*. 2008;9(12):1324-1335.

32 Cubukcu E, Birol, O. Altmışbeş yaş üstü metastatik yumuşak doku sarkom hastalarında pazopanib tedavisinin etkinliğinin retrospektif değerlendirilmesi. *Uludağ Üniversitesi Tıp Fakültesi Dergisi*. 2019;45(1):83-86.

33 Schutz FA, Choueiri TK, Sternberg CN. Pazopanib: Clinical development of a potent anti-angiogenic drug. *Crit Rev Oncol Hematol*. 2011;77(3):163-171.

34 Sleijfer S, van der Graaf WT, Blay JY. Angiogenesis inhibition in non-GIST soft tissue sarcomas. *The Oncologist*. 2008;13(11):1193-1200.

35 DuBois S, Demetri G. Markers of angiogenesis and clinical features in patients with sarcoma. *Cancer*. 2007;109(5):813-819.

36 Tresaugues L, Roos A, Arrowsmith C, et al. Crystal structure of VEGFR1 in complex with N-(4-Chlorophenyl)-2-((pyridin-4-ylmethyl) amino) benzamide. The RCSB PDB. 2013. doi: 10.2210/pdb3hng/pdb

37 Oguro Y, Miyamoto N, Okada K, et al. Design, synthesis, and evaluation of 5-methyl-4-phenoxy-5H-pyrrolo [3, 2-d] pyrimidine derivatives: Novel VEGFR2 kinase inhibitors binding to inactive kinase conformation. *Bioorg Med Chem*. 2010;18(20):7260-7273.

38 Wang Z, Wang X., Li Y., et al. farPPI: A webserver for accurate prediction of protein-ligand binding structures for small-molecule PPI inhibitors by MM/PB (GB) SA methods. *Bioinformatics*. 2019;35(10):1777-1779.

39 Hao GF, Jiang W, Ye YN, et al. ACFIS: A web server for fragment-based drug discovery. *Nucleic Acids Res*. 2016;44(W1):W550-W556.

40 Hao GF, Wang F, Li H, et al. Computational discovery of picomolar Q o site inhibitors of cytochrome bc 1 complex. *J Am Chem Soc*. 2012;134(27):11168-11176.

41 Yang JF, Wang F, Jiang W, et al. PADFrag: A database built for the exploration of bioactive fragment space for drug discovery. *J Chem Inf Model*. 2018;58(9):1725-1730.

42 Cheron N, Jasty N, Shakhnovich EI. OpenGrowth: An automated and rational algorithm for finding new protein ligands. *J Med Chem*. 2016;59(9):4171-4188.

43 Wang E, Sun H, Wang J, et al. End-point binding free energy calculation with MM/PBSA and MM/GBSA: strategies and applications in drug design. *Chem Rev*. 2019;119(16):9478-9508.

44 Pogodin PV, Lagunin AA, Rudik AV, et al. AntiBac-Pred: A web application for predicting antibacterial activity of chemical compounds. *J Chem Inf Model*. 2019;59(11):4513-4518.

45 Brown ED, Wright GD. Antibacterial drug discovery in the resistance era. *Nature*. 2016;529(7586):336-343.

46 Gaulton A, Hersey A, Nowotka M, et al. The ChEMBL database in 2017. *Nucleic Acids Res*. 2017;45(D1):D945-D954.

47 Fourches D, Muratov E, Tropsha A. Curation of chemogenomics data. *Nat Chem Biol*. 2015;11(8):535-535.

48 Pogodin PV, Lagunin AA, Filimonov DA, Poroikov VV. PASS Targets: Ligand-based multi-target computational system based on a public data and naïve Bayes approach. *SAR QSAR Environ Res*. 2015;26(10):783-793.

49 Pogodin PV, Lagunin AA, Rudik AV, et al. How to achieve better results using PASS-Based virtual screening: Case study for kinase inhibitors. *Front Chem*. 2018;6(133):1-14.

50 Filimonov DA, Lagunin AA, Gloriozova TA, et al. Prediction of the biological activity spectra of organic compounds using the PASS online web resource. *Chem Heterocycl Compd*. 2014;50(3):444-457.

51 Zaidi Z, Sharma G, Sahaya Shibu B, et al. In silco prediction of pharmacological properties of the 2-(4-allylpiperazin-1-yl)-1-(1-(4-nitrophenyl)-1h-tetrazol-5-yl) ethanone. *Afr J Biol Sci*. 2024;6:2522-2540.

52 Cadow J, Born J, Manica M, Oskooei A, Rodríguez Martinez M. PaccMann: A web service for interpretable anticancer compound sensitivity prediction. *Nucleic Acids Res*. 2020;48(W1):W502-W508.

53 Kuzu B, Karakuş F. Natural compounds targeting VEGFRs in kidney cancer: An in silico prediction. *JIST*. 2022;12(3):1711-1722.

54 Bharathi D, Boopathy RA. In silico studies on colon cancer against hexadecane, hexadecanoic acid methyl ester and quinoline, 1, 2-dihydro-2, 2, 4-trimethyl compounds from brown seaweed. *IJRPS*. 2020;11(2):1927-1935.

55 Kouassi K, Ganiyou A, Didier D, Benie A, Nahosse Z. In silico docking of rhodanine derivatives and 3D-QSAR study to identify potent prostate cancer inhibitors. *Comput Chem*. 2022;10(2):19-52.

56 Mendie LE, Hemalatha S. Molecular docking of phytochemicals targeting GFRs as therapeutic sites for cancer: An *in silico* study. *Appl Biochem Biotechnol*. 2022;194(1):215-231.

57 Lu SL, Noda T. VEGF (vascular endothelial growth factor) provides antimicrobial effects via autophagy and lysosomal empowerment in endothelial cells. *Autophagy Rep*. 2022;1(1):555-558.

58 Amiri-Kordestani L, Tan AR, Swain SM. Pazopanib for the treatment of breast cancer. *Expert Opin Investig Drugs*. 2012;21(2):217-225.

59 Zhao H, Yang F, Shen W, et al. Pazopanib diminishes non-small cell lung cancer (NSCLC) growth and metastases *in vivo*. *Thorac Cancer*. 2015;6(2):133-140.

60 Roberts JL, Tavallai M, Nourbakhsh A, et al. GRP78/Dna K is a target for Nexavar/Stivarga/Votrient in the treatment of human malignancies, viral infections and bacterial diseases. *J Cell Physiol*. 2015;230(10):2552-2578.

61 Kaur N, Aggarwal AK, Sharma N, Choudhary B. Synthesis and in-vitro antimicrobial activity of pyrimidine derivatives. *Int J Pharm Sci Drug Res*. 2012;4(3):199-204.

62 Abdel-Mohsen HT, Ragab FA, Ramla MM, El Diwani HI. Novel benzimidazole–pyrimidine conjugates as potent antitumor agents. *Eur J Med Chem*. 2010;45(6):2336-2344.

63 Sirisoma N, Kasibhatla S, Nguyen B, et al. Discovery of substituted 4-anilino-2-(2-pyridyl) pyrimidines as a new series of apoptosis inducers using a cell-and

caspase-based high throughput screening assay. Part 1: Structure–activity relationships of the 4-anilino group. *Bioorg Med Chem.* 2006;14(23):7761-7773.

64 Xie F, Zhao H, Zhao L, Lou L, Hu Y. Synthesis and biological evaluation of novel 2, 4, 5-substituted pyrimidine derivatives for anticancer activity. *Bioorg Med Chem Lett.* 2009;19(1):275-278.

65 Kamal A, Dastagiri D, Ramaiah MJ, et al. Synthesis and apoptosis inducing ability of new anilino substituted pyrimidine sulfonamides as potential anticancer agents. *Eur J Med Chem.* 2011;46(12):5817-5824.

66 Pontikis R, Benhida R, Aubertin AM, Grierson DS, Monneret C. Synthesis and anti-HIV activity of novel N-1 side chain-modified analogs of 1-[(2-hydroxyethoxy) methyl]-6-(phenylthio) thymine (HEPT). *J Med Chem.* 1997;40(12):1845-1854.

67 Lu X, Chen Y, Guo Y, et al. The design and synthesis of N-1-alkylated-5-aminoaryalkylsubstituted-6-methyluracils as potential non-nucleoside HIV-1 RT inhibitors. *Bioorg Med Chem.* 2007;15(23):7399-7407.

68 Das K, Clark Jr. AD, Lewi PJ, et al. Roles of conformational and positional adaptability in structure-based design of TMC125-R165335 (etravirine) and related non-nucleoside reverse transcriptase inhibitors that are highly potent and effective against wild-type and drug-resistant HIV-1 variants. *J Med Chem.* 2004;47(10):2550-2560.

69 Summa V, Petrocchi A, Bonelli F, et al. Discovery of raltegravir, a potent, selective orally bioavailable HIV-integrase inhibitor for the treatment of HIV-AIDS infection. *J Med Chem.* 2008;51:5843-5855.

70 Tagat JR, McCombie SW, Nazareno D, et al. Piperazine-based CCR5 antagonists as HIV-1 inhibitors. IV.Discovery of 1-[(4,6-dimethyl-5-pyrimidinyl)carbonyl]-4-[4-[2-methoxy-1(R)-4-(trifluoromethyl)phenyl]ethyl-3(S)-methyl-1-piperazinyl]-4-methylpipe ridine(Sch-417690/Sch-D), a potent, highly selective, and orally bioavailable CCR5 antagonist. *J Med Chem.* 2004;47:2405-2408.

71 Huckova D, Holy A, Masojidkova M, et al. Synthesis and antiviral activity of 2,4-diamino-5-cyano-6-[2-(phosphonomethoxy)ethoxy]pyrimidine and related compounds. *Bioorg Med Chem.* 2004;12(12):3197-3202.

72 Deshmukh MB, Salunkhe SM, Patil DR, Anbhule PV. A novel and efficient one step synthesis of 2-amino-5-cyano-6-hydroxy-4-arylpyrimidines and their anti bacterial activity. *Eur J Med Chem.* 2009;44:2651–2654.

73 Roth B, Strelitz JZ, Rauckman BS. 2,4-Diamino-5-benzylpyrimidines and analogs as antibacterial agents.2.C-Alkylation of pyrimidines with Mannich bases and application to the synthesis of trimethoprim and analogs. *J Med Chem.* 1980;23(3):379-384.

74 Chandrashekaran S, Nagarajan S. Microwave-assisted synthesis and anti-bacterial activity of some 2-Amino-6-aryl-4-(2-thienyl) pyrimidines. *IL Farmaco.* 2005;60:279-282.

75 Mai A, Rotili D, Massa S, et al. Discovery of uracil-based histone deacetylase inhibitors able to reduce acquired antifungal resistance and trailing growth in Candida albicans. *Bioorg Med Chem Lett.* 2007;17:1221-1225.

76 Gholap AR, Toti KS, Shirazi F, Deshpande MV, Srinivasan KV. Efficient synthesis of antifungal pyrimidines via Palladium catalyzed Suzuki/Sonogashira cross-coupling reaction from Biginelli 3,4-dihydropyrimidin-2(1H)-ones. *Tetrahedron*. 2008;64:10214-10223.

77 Ingaral N, Saravanan G, Amutha P, Nagarajan S. Synthesis, in vitro antibacterial and antifungal evaluations of 2-amino-4-(1-naphthyl)-6-arylpyrimidines. *Eur J Med Chem.* 2007;42:517-520.